Dielectrophoresis in Microchips Containing Arrays of Insulating Posts: Theoretical and Experimental Results

Eric B. Cummings* and Anup K. Singh

Chemical & Radiation Detection Laboratories, Sandia National Laboratories, Livermore, California 94551

Dielectrophoresis (DEP), a nonlinear electrokinetic transport mechanism, can be used to concentrate and sort cells, viruses, and particles. To date, microfabricated DEP-based devices have typically used embedded metal electrodes to apply spatially nonuniform, time-varying (AC) electric fields. We have developed an alternative method in which arrays of insulating posts in a channel of a microchip produce the spatially nonuniform fields needed for DEP. Electrodes may be located remotely, allowing operation of the device down to zero frequency (DC) without excessive problems of electrolysis. Applying a sufficiently large electric field across an insulating-post array produces two flow regimes through a competition between electrokinetic flow (combined electrophoresis and electroosmosis) and dielectrophoresis. "Streaming DEP" is observed when DEP dominates diffusion but is overcome by electrokinetic flow. Particles concentrated by DEP forces in areas of electric field extrema travel electrokinetically down the array in flowing streams. In an array of posts, dielectrophoretic forcing within repeated rows adds coherently to produce flowing streams of highly concentrated and rarefied particles. We demonstrate that this reinforcement is a strong function of alignment of the array with respect to the applied electric field and that the particle concentrations can be "enhanced" or "depleted" along columns of posts, enabling a novel class of continuous-flow, selective particle filter/concentrator devices. To our knowledge, this is the first observation of streaming dielectrophoresis. The second regime is "trapping DEP," in which DEP forces dominate over both diffusion and electrokinetic flow, reversibly immobilizing particles on the insulating posts, enabling inexpensive and embedded batch filter/concentrator devices. Devices can be biased electrically to manipulate particles selectively by varying the field strength to vary the relative magnitudes of electrokinetic flow and DEP. Post shapes are contoured easily to control electric field gradients and, hence, DEP behavior. Simple simulations based on similitude of fluid flow and electric field that solve the Laplace equation to obtain fluid velocity have also been developed to predict the dielectrophoretic behavior in an array of posts. These simulations are in excellent agreement with the experimental observations and provide insight into electrokinetic behavior to enable design of dielectrophoretic concentrators and sorters.

Dielectrophoresis (DEP) is the motion of particles toward or away from regions of high electric-field intensity.[1,2] This motion is produced by the action of an electric field on dipole moments induced in the particle and the suspending fluid by the electric field. If the induced dipole moment of the particle is greater than that of the fluid, the particle exhibits "positive dielectrophoresis," experiencing a force toward regions of high electric field intensity. "Negative dielectrophoresis" occurs when the fluid is more polarizable than the suspended particle, and the particles are displaced from high-field regions by the fluid. Dielectrophoresis has captured much interest recently because it is an effective way to trap, manipulate, and separate particles ranging from large DNA strands to blood cells and larger particles in microfabricated devices.[3−16]

In most of the microanalytical devices for genomics[17−21] and proetomics,[22−24] samples to be analyzed are reasonably pure mixtures of DNA or proteins, with steps to clean up, such as cell

* To whom correspondence should be addressed. Phone: 925-294-2385. Fax: 925-294-3020. E-mail address: ebcummi@sandia.gov.

(1) Jones, T. B. *Electromechanics of Particles*; Cambridge University Press: Cambridge, 1995.
(2) Pohl, H. A. *Dieletrophoresis*; Cambridge University Press: Cambridge, 1978.
(3) Gascoyne, P. R. C.; Huang, Y.; Pethig, R.; Vykoukal, J.; Becker, F. F. *Meas. Sci. Technol.* **1992**, *3*, 439−445.
(4) Gascoyne, P. R. C.; Huang, Y.; Wang, X. B.; Becker, F. F. *Biophys. J.* **1994**, *66*, A238-A238.
(5) Gascoyne, P. R. C.; Vykoukal, J. *Electrophoresis* **2002**, *23*, 1973−1983.
(6) Gascoyne, P. R. C.; Huang, Y.; Vykoukal, J.; Becker, F. F.; Wang, X. B. *Biophys. J.* **1997**, *72*, WPME2−WPME2.
(7) Pethig, R.; Huang, Y.; Wang, X. B.; Burt, J. P. H. *J. Phys. D: Appl. Phys.* **1992**, *25*, 881−888.
(8) Pethig, R.; Markx, G. H. *Trends Biotechnol.* **1997**, *15*, 426−432.
(9) Wang, X. B.; Yang, J.; Huang, Y.; Vykoukal, J.; Becker, F. F.; Gascoyne, P. R. C. *Anal. Chem.* **2000**, *72*, 832−839.
(10) Becker, F. F.; Wang, X. B.; Huang, Y.; Pethig, R.; Vykoukal, J.; Gascoyne, P. R. C. *Proc. Natl. Acad. Sci. U.S.A.* **1995**, *92*, 860−864.
(11) Cheng, J.; Sheldon, E. L.; Wu, L.; Heller, M. J.; O'Connell, J. P. *Anal. Chem.* **1998**, *70*, 2321−2326.
(12) Cheng, J.; Sheldon, E. L.; Wu, L.; Uribe, A.; Gerrue, L. O.; Carrino, J.; Heller, M. J.; O'Connell, J. P. *Nat. Biotechnol.* **1998**, *16*, 541−546.
(13) Fiedler, S.; Shirley, S. G.; Schnelle, T.; Fuhr, G. *Anal. Chem.* **1998**, *70*, 1909−1915.
(14) Muller, T.; Gerardino, A.; Schnelle, T.; Shirley, S.; Bordoni, F.; DeGasperis, G.; Leoni, R.; Fuhr, G. *J. Phys. D: Appl. Phys.* **1996**, *29*, 340−349.
(15) Green, N.; Morgan, H. *J. Phys. D: Appl. Phys.* **1997**, *30*, 2626−2633.
(16) Schnelle, T.; Muller, T.; Gradl, G.; Shirley, S.; Fuhr, G. *Electrophoresis* **2000**, *21*, 66−73.
(17) Effenhauser, C. S.; Paulus, A.; Manz, A.; Widmer, H. M. *Anal. Chem.* **1994**, *66*, 2949−2953.

10.1021/ac0340612 CCC: $25.00
Published on Web 00/00/0000

isolation and sorting, being performed off-chip using macroscale techniques such as centrifugation or cytometry. In attempting to develop micro total analysis systems (μTAS), it is desirable for cell-manipulation steps to be integrated at chip scales. DEP is an extremely effective means of manipulating particles of diameters between 100 nm and 10 μm and offers an excellent choice for separation, isolation, and concentration of cells. Most implementations of dielectrophoresis utilize embedded electrodes to produce the necessary electric-field gradients. Moreover, the applied fields are nearly always purely high-frequency alternating current (AC) to avoid gas generation and eliminate electroosmosis and electrophoresis.

In this study, we present measurements of constant-voltage (DC) dielectrophoretic effects on particle concentration in electrically driven flows through uniformly patterned arrays of insulating posts. Use of DC electric fields allows for finer manipulation of particles, because one can manipulate the relative magnitudes of electrokinetic flow (which includes both electrophoresis and electroosmosis) and DEP. The particle flows in chips with arrays of insulating posts exhibit two striking phenomena: dielectrophoretic "streaming", in which streams of fluid having low and high particle concentration flow through the arrays, and "trapping", in which particles are reversibly immobilized on the insulating posts. Streaming occurs when DEP overcomes diffusion and is slightly weaker than electrokinetic flow or advection; trapping occurs when dielectrophoresis overcomes diffusion, electrokinetic flow, and advection. We observe a dramatic dependence of the patterns of streaming and trapping on the orientation of arrays with respect to the mean applied electric field and on the shape of the posts in the arrays. Use of insulating material provides a number of other advantages over devices that need deposited metal electrodes, including fabrication by stamping, etching, or molding that are simpler and cheaper than depositing metal electrodes onto microchannel surfaces.[25−27] Insulators are also less susceptible to fouling than electrodes, and do not electrochemically alter the fluid or particles (e.g., generation of gas bubbles).

Simulations based on similitude of fluid velocity and electric field were also developed to predict the particle transport in the array of posts. Typically, one has to solve coupled Poisson and Navier−Stokes equations for direct numerical simulation of electrokinetic flow[28,29] and dielectrophoresis. The problem can be simplified to a great extent by taking advantage of the fact that fluid velocity is proportional to the electric field, and hence, both the electric potential and fluid flow can be computed by solving only the Laplace equation for electric potential.[25] The particle concentration gradients predicted by the simple potential flow solver were in excellent agreement with the experimental observations. Consequently, it can be used to design and optimize DEP-based devices without resorting to trial-and-error experimentation or complicated computational methods.

THEORY

An electric field having a DC component applied to a conductive-liquid-filled microchannel generally produces electroosmosis and electrophoresis. Electroosmosis is flow produced by an electric field acting on the net mobile charge in the fluid within the electric double layer surrounding the charged surface of the microchannel.[30,31] Intimately related, electrophoresis is the transport of mobile charged ionic species under an applied electric field. Both electroosmotic and electrophoretic transport are linearly proportional to the local electric field, and the superposition of these can be termed as electrokinetic flow. Ideal electrokinetic flow is a special limiting case of the combined transport in which the electrokinetic velocity field (u_{ek}) is everywhere proportional to the local electric field (E), as given by

$$u_{ek} = \mu_{ek}E = u_{eo} + u_{ep} = (\mu_{eo} - \mu_{ep})E \qquad (1)$$

where μ_{ek}, μ_{eo}, and μ_{ep} are the electrokinetic, electroosmotic, and electrophoretic mobility, respectively. In ideal electrokinetic flow, particles flow along *electric field lines*. Ideal electrokinetic flow can neither concentrate nor deplete particles in an initially uniform distribution.

Dielectrophoretic velocity, u_{dep}, is proportional to the gradient of the dot product of the electric field,[2]

$$u_{dep} = \mu_{dep}\nabla(E\cdot E) \qquad (2)$$

where μ_{dep} is the dielectrophoretic mobility.

Unlike electrokinetic flow, dielectrophoretic motion is along *electric field gradients* and can concentrate and rarefy particles. Such electric field gradients are produced when obstacles such as insulating posts are located within a flow channel having an applied electric field (in AC dielectrophoresis, the gradients are produced by embedded electrodes). The resulting nonuniform electric field drives dielectrophoresis of molecules and particles, which differ in polarizability from the suspending liquid. The latex particles used in this study are more polarizable at DC than the 1 mM phosphate buffer. Consequently, the dipole moment of particles aligns parallel to the electric field, and particles are drawn to the field maximum (positive dielectrophoresis).

For dilute, creeping flow in insulating channels, the flux of particles, j, including diffusion, advection, electrokinetic flow, and dielectrophoresis is

$$j = -D\nabla c + c[u + u_{ek} + u_{dep}] \qquad (3)$$

where D is the diffusivity, c is the concentration of the particles, and u is nonelectrokinetic component of velocity. The continuity

(18) Sanders, G. H. W.; Manz, A. *TrAC−Trends Anal. Chem.* **2000**, *19*, 364−378.
(19) Woolley, A. T.; Mathies, R. A. *Proc. Natl. Acad. Sci. U.S.A.* **1994**, *91*, 11348−11352.
(20) Mathies, R. A.; Huang, X. C. *Nature* **1992**, *359*, 167−169.
(21) Paegel, B. M.; Emrich, C. A.; Weyemayer, G. J.; Scherer, J. R.; Mathies, R. A. *Proc. Natl. Acad. Sci. U.S.A.* **2002**, *99*, 574−579.
(22) Li, J. J.; Thibault, P.; Bings, N. H.; Skinner, C. D.; Wang, C.; Colyer, C.; Harrison, J. *Anal. Chem.* **1999**, *71*, 3036−3045.
(23) Liu, Y. J.; Foote, R. S.; Jacobson, S. C.; Ramsey, R. S.; Ramsey, J. M. *Anal. Chem.* **2000**, *72*, 4608−4613.
(24) Throckmorton, D. J.; Shepodd, T. J.; Singh, A. K. *Anal. Chem.* **2002**, *74*, 784−789.
(25) Cummings, E. B.; Griffiths, S. K.; Nilson, R. H.; Paul, P. H. *Anal. Chem.* **2000**, *72*, 2526−2532.
(26) Cummings, E. B.; Singh, A. K. *Proc. SPIE* **2000**, *4177*, 164−173.
(27) Chou, C. F.; Tegenfeldt, J. O.; Bakajin, O.; Chan, S. S.; Cox, E. C.; Darnton, N.; Duke, T.; Austin, R. H. *Biophys. J.* **2002**, *83*, 2170−2179.
(28) Pantankar, N. A.; Hu, H. H. *Anal. Chem.* **1998**, *70*, 1870−1881.
(29) Ermakov, S. V.; Jacobson, S. C.; Ramsey, J. M. *Anal. Chem.* **1998**, *70*, 4494−4504.

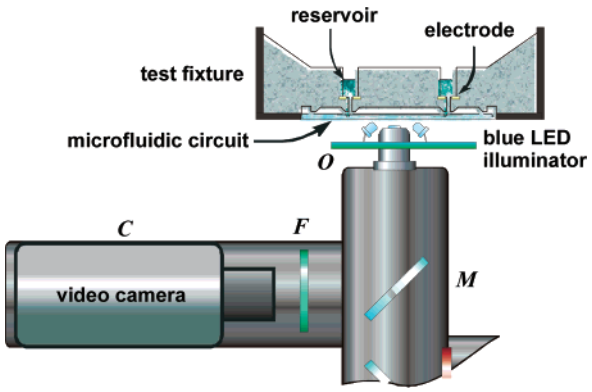

Figure 1. Schematic of the experimental setup for imaging dielectrophoresis.

equation (eq 4) provides the initial change of concentration with time before a steady state is reached.

$$\frac{\partial c}{\partial t} = \nabla \cdot j \tag{4}$$

Different flow regimes can exist for cases in which DEP and electrokinetic flow are present together. Because dielectrophoretic transport is of second order in the applied electric field, it is negligible compared to electrokinetic flow (or advection) and diffusion at suitably low applied fields. In this regime, no appreciable spontaneous particle concentration gradients form; existing gradients diffuse and disperse.

Above a thresold applied electric field, dielectrophoresis begins to overcome diffusion but cannot overcome electrokinetic flow. Filaments of concentrated and rarefied particles appear along flow streamlines. This flow regime can be called "streaming dielectrophoresis." The concentration and rarefaction from streaming dielectrophoresis becomes more pronounced until above a higher threshold applied field, dielectrophoresis overwhelms electrokinesis as well as diffusion. In this regime, particles are trapped dielectrophoretically and can be concentrated to nearly solid density. This regime is called "trapping dielectrophoresis".

EXPERIMENTAL SECTION

Apparatus. The experimental apparatus is shown schematically in Figure 1.[32] Experiments were conducted in a microfluidic chip consisting of patterned channels isotropically etched in glass with a thermally bonded glass cover. The microfluidic chip was reversibly sealed to a test fixture via a vacuum chuck. This PDMS fixture provides 16 open, 1-mL fluid reservoirs with embedded gold ring electrodes. A high-voltage power supply (Stanford Research Systems, PS350) was used to apply electric fields. To minimize hazards associated with high voltages, the entire experimental setup was encased in a plexiglass enclosure that was interlocked. The microflow was imaged by an LED-illuminated, inverted, three-video-camera epifluorescence microscope. A ring of 24 blue LEDs (Nichia, NSPB300A) flood illuminated the sample with light having a peak wavelength of 470 nm. A 10× microscope objective (O) imaged a ~520 × 390 μm region of the circuit onto camera C. Dichroic mirror M reflected fluorescence in the wavelength range below ~550 nm into an emission filter F which further limited the signal wavelength range to 500−530 nm. The filtered signal fell onto a video-rate monochromatic 1/2-in. CCD camera (Cohu 4910, C). The RS-170 output of the video camera was digitized to 8 bits by a frame grabber (Matrox Meteor) and recorded directly to a computer disk. The images were interlaced at 640 × 480-pixel resolution, with each interlaced field temporally separated by 16.7 ms.

Microchip for Dielectrophoresis. The glass microchip had 7-μm-deep channels containing uniform arrays of diamond, square, and circular posts at different angles with respect to the applied electric field. The diamond and square posts were 36 μm on a side on 63 μm centers. The circular posts were 33 μm in diameter, also on 63 μm centers.

The microchip was fabricated from Schott D263 glass wafers (100-mm diameter, 1.1 mm thickness) using standard photolithography, wet etch, and bonding techniques.[24] Briefly, glass wafers were sputtered with chrome (200 nm) that served as the hard mask. A 1.2-μm-thick layer of OCG 825 (Arch Chemical Co., Columbus, OH) positive photoresist was spin-coated and soft-baked (90 °C, 5 min). The mask pattern was transferred to the photoresist by exposing it to UV light in a contact mask aligner at 80 mJ/cm^2. After exposure, the photoresist was developed with OCG 934 2:1 developer and hard-baked (120 °C, 30 min). Exposed chrome was etched with CEN 300 Micro-chrome etchant (Microchrome Technologies Inc., San Jose, CA), and the subsequently exposed glass was etched with a 25% HF solution. Access holes were drilled in the cover plate (D263) with diamond-tipped drill bits. The etched wafers and cover plates were cleaned with 4:1 H_2SO_4/H_2O_2 (100 °C) and then 1:5:1 $NH_4OH/H_2O/H_2O_2$ (75 °C); they were then rinsed in a cascade bath followed by a spin rinse dry; and finally, they were aligned and thermally bonded at 610 °C in a N_2-purged programmable furnace.

DEP Experiments. The microchip was rinsed vigorously with 0.1 M NaOH, deionized water, and buffer before use to remove any surface-adsorbed contaminants. The holes in the chip were aligned with the manifold and the desired channel, and corresponding reservoirs were filled with equal volumes of 1 mM phosphate buffer, pH 7.7. Carboxylated latex nanospheres (Molecular Probes yellow-green, 200-nm, carboxylate-modified fluospheres) were used as model particles for dielectrophoresis. These neutrally buoyant nanospheres (density = 1.05 g cm^{-3}) are labeled with a highly fluorescent dye similar to fluorescein (1.1 × 10^5 fluorescein equivalents per particle). Hydrodynamic diameters of microspheres were estimated by dynamic light scattering (DLS) using a commercial device (Zeta Plus, Brookhaven Instruments Corp). Samples for size measurement were prepared by adding 10 μL of beads to 2 mL of deionized water. The bead suspension was sonicated for 15 min to break up agglomerates. Measurements were performed at a 90° scattering angle using a 633-nm diode laser, and a correlation function was generated by a BI-9000AT digital correlator. The data were analyzed using the constrained regularization method to yield a hydrodynamic diameter of 192.3 ± 5.3 nm. The ζ potential of the bead suspension was measured by electrophoretic light scattering (ZetaPlus,

(30) Rice, C. L.; Whitehead, R. *J. Phys. Chem.* **1965**, *69*, 186−203.
(31) Probstein, R. F. *Physicochemical Hydrodynamics*; John Wiley: New York, 1995.
(32) Singh, A. K.; Cummings, E. B.; Throckmorton, D. J. *Anal. Chem.* **2001**, *73*, 1057−1061.

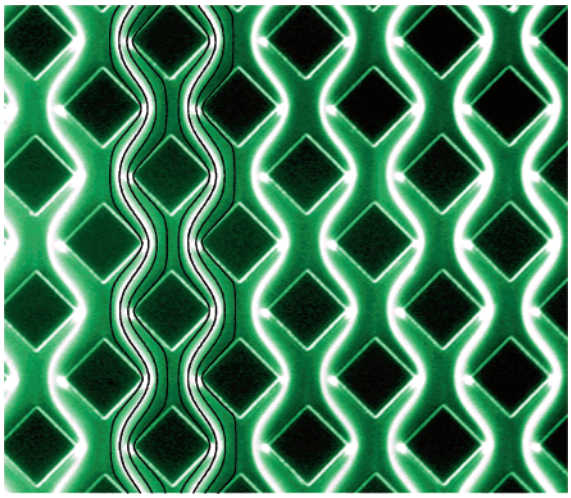

Figure 2. Fluorescence image of streaming dielectrophoresis of 200-nm fluorescent latex spheres (white) in a microchip containing an array of diamond-shaped posts (black). The glass microchannel is 7 μm deep and consists of an array of 36-μm-square posts (the black diamonds) with 63-μm spacing between centers. The DC electric field (80 V/mm) and resulting electroosmotic flow are from top to bottom. The black lines indicate streamlines predicted using simulations. The bright spots at the left and right tips of the posts are regions of trapping dielectrophoresis.

Brookhaven Instruments) that is based on the scattering of light from particles that move in a liquid under the influence of an applied electric field. Beads diluted in a 10 mM KCl solution had a ζ potential of -19 ± 2.6 mV. The permittivity and conductace of latex spheres has been reported as 2.5 and 18.5 mS/m.[15]

The beads were diluted 100- to 1000-fold in 1 mM phosphate buffer (and sonicated extensively to break up aggregates before addition to the channels. The dielectrophoresis was initiated by applying high voltage across selected channels. Videos of the resulting motion of fluorescent nanospheres were taken using an inverted epifluorescence microscope.

SIMULATIONS

Under the experimental conditions used here (Debye layer thickness $\ll$ channel dimensions), the electrokinetic flow is proportional to the local electric field. This allows us to determine the flow field directly from solving the Laplace equation ($\nabla^2\phi = 0$) governing electric potential, without solving the coupled momentum transport (Navier−Stokes) and Poisson equations.[25] Appendix A describes the potential flow solver called "Laplace" that has been developed for carrying out the simulation results presented in later sections. In addition to elucidating the electric field-induced flows observed experimentally, the potential flow solver also provides useful insight for designing microchips to carry out dielectrophoresis and other electrokinetic effects.

RESULTS AND DISCUSSION

Streaming Dielectrophoresis. Figure 2 shows the fluorescence image of a flow in a glass microchannel containing an array of diamond posts. The array is 56 posts long (in the flow direction) and 16 posts wide. The electric field (80 V/mm) is applied from top to bottom, generating an electroosmotic flow in the same direction. The liquid in the channels is 1 mM phosphate buffer containing a dilute solution of 200-nm latex particles. Sedimentation can be ignored on the experimental time scale, since the particles are neutrally buoyant. The images are ~1-s time averages. The grayscale of the image shows the relative intensity of the particle fluorescence and is, thus, a measure of the concentration of the particles. The thin, bright border around each post is strong specular reflection of the illumination leaking through the color filters and is not a fluorescence signal.

The collinear alignment of the diamond-shaped posts with respect to the electric field creates a field maximum at the left and right vertexes and a minimum at the top and the bottom vertexes. The solid curves represent the ideal electrokinetic streamlines produced using potential flow simulations described in Appendix A. Particles, because they have a positive dielectrophoretic mobility, are drawn to the field maximums and follow streamlines along the alternating left and right vertexes of the posts. The streamlines along the centers of the posts have the lowest concentration of particles. Except immediately at the left and right vertexes of the posts, the field is not sufficiently strong to trap the particles; therefore, they flow electrokinetically and appear as streams of concentrated particles moving along a column of posts. These streams of particles become more concentrated as they travel downstream because of a coherent reinforcement of the dielectrophoretic transport along repeated rows of posts. The small bright regions near the left and right vertexes of the posts show zones of trapping dielectrophoresis produced by the strong local field concentration.

Figure 2 illustrates the ability of streaming dielectrophoresis to concentrate particles, such as cells, in a continuous-flow device. A particle concentrator can be devised readily by designing collection channels downstream of such an array of posts. By constructing posts in the same step as the rest of the microfluidic channels, this type of concentrator can be integrated into microanalytical systems, including systems to analyze protein/genomic contents of individual or groups of cells, or a microcytometer.

Figure 2 also shows that filaments on the left side of the array are less focused than those on the right. This is due to slight misalignment (0.3°) of electric field lines with the vertical diagonals of the diamond posts. The extent of concentration (or rarefaction) by streaming dielectrophoresis in an array of posts is a very strong function of coherent reinforcement of DEP effect by consecutive rows and columns. In Figure 2, the streamline pattern approximately repeats after an offset of 1 row and 1 column, leading to strong cumulative DEP effect. If the array angle is changed relative to the applied electric field, there is a drastic change in the overall DEP behavior, as shown in Figure 3. The array, field-strength, and all other experimental conditions are identical to those in Figure 2, except that the columns of the array are oriented at 20.5° relative to the electric field. In this flow, the variation in concentration is much weaker because of the limited cooperative effect of the posts as streamline patterns approximately repeat after an offset of 5 rows and 2 columns (rather than the offset of approximately 1 row in Figure 2).

Figure 4 shows the observed streaming DEP behavior in an array of squares oriented at ~1.6° (Figure 4a) and ~3.2° (Figure 4b) with respect to the applied electric field (aligned vertically in the figure). In Figure 4a, this angle of attack produces filaments or streams that are slightly asymmetrical with respect to the post

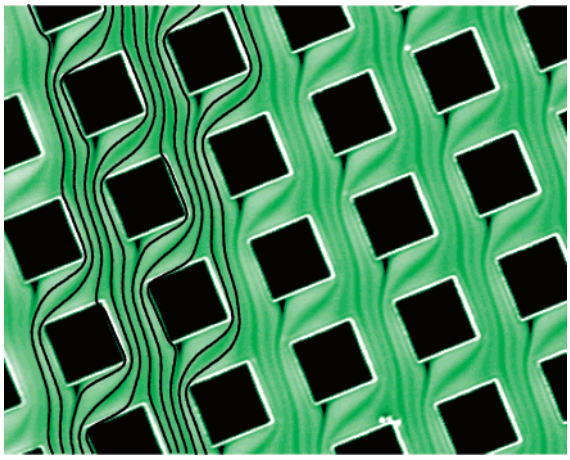

Figure 3. Effect of post array alignment with electric field on streaming dielectrophoresis. Streaming dielectrophoresis is carried out at the same conditions as in Figure 2, except the electric field is oriented at 20.5° relative to the post columns. The concentration of particles is significantly weaker because dielectrophoresis is not reinforced effectively by the array.

columns. Again, the streams align with the calculated electrokinetic flow streamlines, and the array coherently reinforces DEP. Particles are highly depleted from the electric field minimums in the large stagnant regions of the flow between the posts, which act like repulsive dielectrophoretic potential barriers. Field concentrations at the vertexes of the posts span such short distances and the flow in these concentrations is so rapid that simulations indicate significant nonequilibrium polarization, and electrorotation effects reduce their ability to attract the positive-dielectrophoretic particles. Consequently, while the particles are alternately attracted and repelled from the columns, the repulsive forces have the greater effect, producing the observed depletion. Figure 4b shows the effect of rotating the array further from the applied field. The stream asymmetry is more pronounced as particles are repelled from the potential barriers in the near-stagnant region up- and downstream from the posts, significantly concentrating the particles to the left of the post and completely filtering particles from the fluid at the right of the posts. Such arrays can be said to be operating in a "depletion mode", in which the concentration of particles is depleted along the columns. The depleted streams retain their distinction, even after the last row of posts, because the flow is laminar.

Changing the shape of posts changes the electric field gradients and flow patterns, consequently changing the balance of attraction and repulsion that produces streaming DEP. Figure 5a shows the particle-fluorescence image of a streaming DEP flow in an array of circular posts. The posts are 33 μm in diameter with center-to-center spacing of 63 μm. The electric field (25 V/mm) is applied directly along the axis of the vertical array. Particles are repelled from the stagnant regions at the upstream and downstream sides of the posts, evidenced by the modest fluorescence dip in these regions. However, the extent of the stagnation region and residence time through its repulsive field is much smaller than that for Figure 4. The long residence time and large spatial extent of the field concentrations on the sides of the posts produces a strong attractive effect and minimal polarization nonequilibrium. The net effect of the decreased repulsion and enhanced attraction to the post columns is an enhancement of the particle concentration along the post columns. In contrast to the arrays in Figure 4, this array can be said to be operating in an "enhancement mode".

Figures 4 and 5 clearly show that streaming DEP is sensitive to post shape. Numerical modeling has been performed to support this assertion and understand the underlying effects. Figure 5b shows a numerical simulation of combined electrokinesis, dielectrophoresis, and diffusion of particles in an array of circular posts at 0° incidence. The simulation was performed using a quasi-two-dimensional ideal electrokinetic transport solver and Monte Carlo particle motion simulator (see Appendix A and B). The enhancement effect of the circular posts is evident in the concentration of the black streaks, which show the particle trajectories. The spectral color map in the background depicts the combined electrokinetic and dielectrophoretic speed field. The highest speeds are blue, and zero speed is red. Particles are introduced at uniform stream-function spacing at the top of the figure, and the electrokinetic flow is from top to bottom. The simulation results are in very good agreement with the experimental results

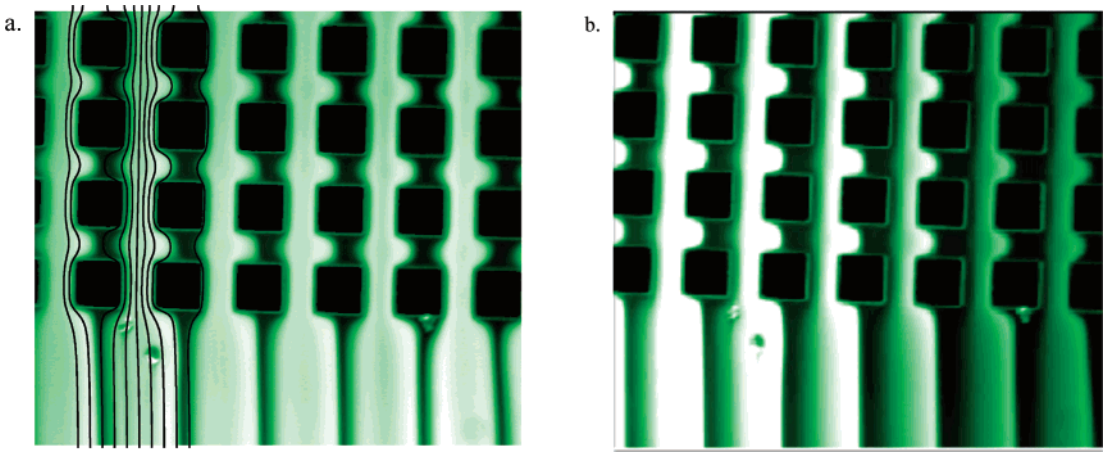

Figure 4. Streaming dielectrophoresis of fluorescent latex spheres in an array of square posts. The field (80 V/mm) is from top to bottom. (a) Electric field is oriented at ~2° with respect to the post columns. Particles are significantly depleted along the post columns. (b) Electric field is oriented at ~3° with respect to the post columns. Particles are depleted between the posts, concentrating on the left side of each column. The concentration gradient across the array shows the cumulative effect of depletion. Concentrated particle bands are maintained even beyond the end of the array because of laminar flow.

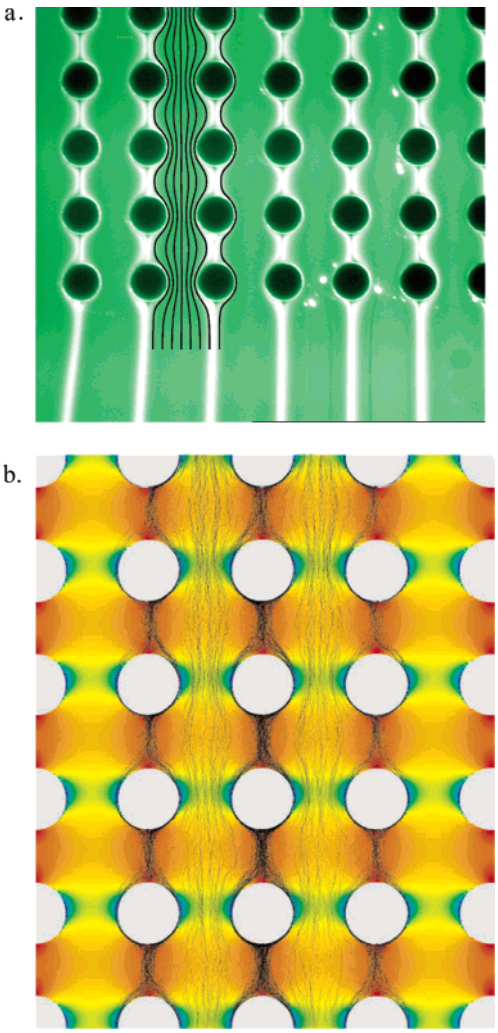

Figure 5. (a) Effect of post shape on streaming dielectrophoresis. Unlike Figures 3 and 4, the particles concentrate in the region along the post columns in an array of circular posts (33-μm diameter on 63-μm centers). The dielectrophoretic enhancement or depletion of particles can be easily tuned by changing the shape of posts. The electric field (25 V/mm) and electroosmotic flow are from top to bottom. (b) Continuum and particle simulation of combined electrokinetic flow, dielectrophoresis, and diffusion in an array of circular posts showing particle concentration along the posts. The background color depicts the mean particle speed: red and blue indicate zero and the highest speed, respectively.

(Figure 5a), indicating that 2-dimensional potential-flow solver performs adequately in calculating flow behavior. The simulation capability enables design and geometrical optimizatiom of arrays for enhancement or depletion mode behavior.

Figure 6 shows eight simulations of monodisperse particles with different dielectrophoretic mobilities (arbitrary units) ranging from negative at the left to neutral at the center to positive at the right. Again, the background spectral color map depicts the combined electrokinetic and DEP speed. Regions of maximum speed in a simulation appear in blue, and comparatively low-speed regions appear red. The absolute scales are different for each simulation. The applied electric field has a slope of 10%. Particles having zero DEP mobility follow the applied electric field. Particles having a modest positive mobility are attracted to the columns of posts (enhancement). The 10% cross-flow advects the particles to collect in streams on the leeward side of the posts. Within a range

Figure 6. Continuum and particle simulation of combined electrokinetic flow, dielectrophoresis, and diffusion in an array of circular posts for particles having different dielectrophoretic mobilities. The background color map is the same as Figure 5b. Particles with zero DEP mobility follow the electric field (and electrokinetic flow) that has a slope of 10%. Particles with positive DEP mobility are attracted (enhancement) to the post columns (same as in Figure 5), while particles with negative DEP mobility are repelled (depletion) by the large field gradients at the posts. Particles with high DEP mobility get trapped.

of mobilities, streaming DEP causes particles to follow the columns of posts, not the electric field, facilitating both selective continuous-flow concentration and filtration. At the right, the particle mobility is sufficiently high to induce trapping. The same array works in depletion mode for particles having a negative DEP mobility, as shown by the images at left. Such particles are repelled by the large field concentration at the side of the posts and are attracted to the small field null at the top and bottom of the posts. The particles follow columns of posts, this time on the windward side, over a considerably larger range in mobilities than for positive-mobility particles. However, the transition from streaming to trapping DEP occurs over a comparably narrow range in mobility. Depletion-mode devices appear in simulations to be more robust and operate over a significantly wider range than their enhancement-mode counterparts. Their decreased sensitivity to surface flaws—particles tend to be repelled from surfaces—will probably favor depletion-mode devices further.

Trapping Dielectrophoresis. At relatively high electric fields, dielectrophoresis overcomes electrokinesis, advection, diffusion, and electrostatic repulsion to concentrate and trap particles. Figure 7 shows steady-state trapping dielectrophoresis. The zones of bright fluorescence contain particles that are concentrated to near solid density and are relatively immobile. Weaker streaming dielectrophoresis is also evident. In steady state, the traps are filled with particles to capacity, limited by the potential well depth and extent. The shape and depth of the trapping potential well is generally affected by perturbations of the electrokinetic flow, and viscosity, by the partly and wholly immobilized particles and perturbations of the flow boundaries. However, a simple model

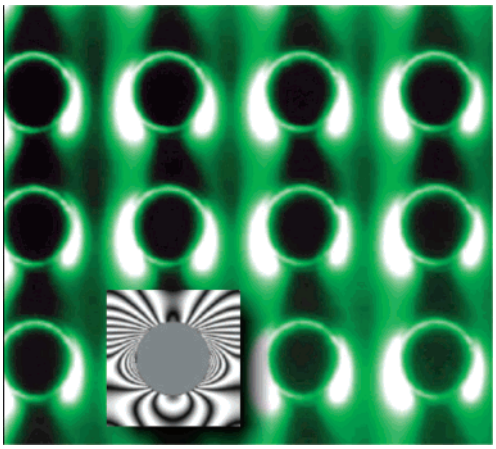

Figure 7. Trapping dielectrophoresis of particles at high applied electric fields. The electric field of 100 V/mm is applied from top to bottom in an array of circular posts (33-μm diameter on 63-μm centers). The overlayed picture shows the simulated isopotentials experienced by particles. Regions where isopotentials curve back onto a post are dielectrophoretic traps.

of the trapping potential that neglects these complications captures the general nature of the trapped regions. The combined electrokinetic and dielectrophoretic potential, $\mu\phi - \nu(E \cdot E)$ (μ and ν are electrokinetic and dielectrophoretic mobility, respectively), and potential within an array of circular posts is overlayed in Figure 7 as a simulated interferogram in which fringes correspond to isopotentials. This simplifed theory strictly applies before particle concentration gradients form. The regions on the lower left and right of the posts where fringes begin and end are potential wells for positive dielectrophoretic particles. Traps for negative dielectrophoretic particles also appear at the top and bottom of the post. The number of fringes in these potential wells shows that the depth of the negative dielectrophoretic trap is much smaller than that of the positive dielectrophoretic traps.

CONCLUSIONS

Dielectrophoresis using insulating posts in DC electric fields revealed different regimes of electrokinetically driven particle transport not previously reported. These regimes result from the interplay of dielectrophoretic and electrokinetic (combined electroosmotic and electrophoretic) forces on particles. At the lowest electric field, dielectrophoresis is too small compared to electrokinetic flow. At moderate applied electric fields, dielectrophoresis overwhelms diffusion and electrostatic repulsion among the particles but not electrokinetic flow, resulting in streams of concentrated and rarefied particles. At higher applied fields, dielectrophoresis dominates over other transport mechanisms, trapping particles at field maximums. Streaming dielectrophoresis can be coherently reinforced within a patterned array of posts to produce highly concentrated or rarefied streams of particles. These effects enable a new class of continuous-flow dielectrophoretic particle filter/concentrators that can be used for biological applications. Simple mathematical models and continuum simulations based on ideal electrokinetic flow and dielectrophoresis that can be used to design novel dielectrophoretic concentrators and sorters were also developed.

ACKNOWLEDGMENT

This work was financially supported by Laboratory Directed Research and Development program at Sandia National Laboratories. Sandia is a multiprogram laboratory operated by Sandia Corporation, a Lockheed Martin Company, for the United States Department of Energy under contract DE-AC04-94AL85000.

APPENDIX A: POTENTIAL FLOW SOLVER "LAPLACE"

Two-dimensional simulations were accomplished using the "Laplace" code, (Cummings, SAND report) which is a general-purpose simulator for ideal electrokinetic flow. The software solves the modified Laplace equation $\sigma(x, y)\nabla\varphi(x, y) = 0$ for the velocity/electrostatic potential φ on a quasiplanar domain that is specified in a bitmapped image file through the field σ. The uniform, square, finite-difference computational grid is generated automatically from a tagged image file (TIFF) bitmap whose blue channel conveys the permeability $\sigma(x, y)$ of the channel across the image. The blue channel is an eight-bit value for each pixel with values of 0×00 and $0 \times$ FF corresponding to a channel of zero permeability (a wall) and a channel of smallest possible permeability (for a given design), respectively. The solution is an exact discretization for ideal electrokinesis, provided the depth of the channel does not vary along any streamlines. The discretization method enables variable-depth channel geometries to be input easily using drawing programs and CAD software. Once the flow fields have been obtained, particles are "injected" and traced during postprocessing of the solution. Each particle has a vector location, velocity, scalar elapsed time, propagated distance, starting potential, and current potential, among other integrated local properties. When a particle propagates, the software updates its properties according to the bilinearly interpolated values of the fields at its location.

APPENDIX B: SIMULATION OF FLOW IN AN ARRAY OF CIRCULAR POSTS (FIGURE 5)

The electric field in a unit cell of the array is obtained by solving the Laplace equation with periodic boundary conditions. The unit cell solution is an exact solution for the electric field in a spatially infinite array of posts and is generally accurate within the interior of arrays of posts of even modest extent (fewer than 10 posts on a side). The ideal electrokinetic velocity field is simply the product of this field with a scalar electrokinetic mobility. Next, Laplace directly simulates the motion of point tracer particles within this infinite domain. A large number of particles (typically $100-10^4$) are introduced to the system at edges of the unit cell spaced so that constant volumetric flux flows between them. The instantaneous velocity of each particle is calculated by adding the

(1) electrokinetic velocity obtained from the product of the electrokinetic mobility and electric field at the instantaneous location of the particle (bilinearly interpolated between grid points),

(2) DEP velocity obtained from the product of the DEP mobility and the gradient of the square of the electric field, and

(3) diffusional velocity obtained from the product of the square root of the diffusivity with a pseudorandom number.

The displacement of the particle for each discrete time step is the product of the resulting velocity and a small time-step parameter. This displacement is added to the instantaneous particle position, and the propagation procedure repeats.

The simulations are simple to perform but ignore interparticle forces and finite-particle-size effects. Moreover, the procedure ignores more complicated effects, such as how immobilized or

partially immobilized particles having a different surface charge density than the channel surface produce vorticity and nonideal electrokinetic behavior; how dense collections of particles can affect the viscosity, dielectric constant, and electric field; etc. Finally, for clarity and simplicity, the simulations assume equilibrium polarization. The simplified transport resulting from this set of simplifying approximations can be called "linear dielectrophoresis." In short, "linear dielectrophoresis" assumes that the presence or absence of a particle has no influence on any other particle or field.

Received for review January 22, 2003. Accepted June 7, 2003.

AC0340612